7502–7517 *Nucleic Acids Research, 2019, Vol. 47, No. 14* *Published online 21 June 2019*
doi: 10.1093/nar/gkz542

Quantitative proteomics revealed C6orf203/MTRES1 as a factor preventing stress-induced transcription deficiency in human mitochondria

Anna V. Kotrys [1], Dominik Cysewski [1], Sylwia D. Czarnomska [1], Zbigniew Pietras[1,2], Lukasz S. Borowski [1,3], Andrzej Dziembowski [1,3] and Roman J. Szczesny [1,*]

[1]Institute of Biochemistry and Biophysics Polish Academy of Sciences, Warsaw 02-106, Poland, [2]Laboratory of Protein Structure, International Institute of Molecular and Cell Biology, Warsaw 02-109, Poland and [3]Faculty of Biology, Institute of Genetics and Biotechnology, University of Warsaw, Warsaw 02-106, Poland

Received February 04, 2019; Revised June 05, 2019; Editorial Decision June 06, 2019; Accepted June 13, 2019

ABSTRACT

Maintenance of mitochondrial gene expression is crucial for cellular homeostasis. Stress conditions may lead to a temporary reduction of mitochondrial genome copy number, raising the risk of insufficient expression of mitochondrial encoded genes. Little is known how compensatory mechanisms operate to maintain proper mitochondrial transcripts levels upon disturbed transcription and which proteins are involved in them. Here we performed a quantitative proteomic screen to search for proteins that sustain expression of mtDNA under stress conditions. Analysis of stress-induced changes of the human mitochondrial proteome led to the identification of several proteins with poorly defined functions among which we focused on C6orf203, which we named MTRES1 (*Mitochondrial Transcription Rescue Factor* 1). We found that the level of MTRES1 is elevated in cells under stress and we show that this upregulation of MTRES1 prevents mitochondrial transcript loss under perturbed mitochondrial gene expression. This protective effect depends on the RNA binding activity of MTRES1. Functional analysis revealed that MTRES1 associates with mitochondrial RNA polymerase POLRMT and acts by increasing mitochondrial transcription, without changing the stability of mitochondrial RNAs. We propose that MTRES1 is an example of a protein that protects the cell from mitochondrial RNA loss during stress.

INTRODUCTION

Mitochondria play an important role in cell homeostasis and their dysfunction is associated with numerous pathological states in humans (1). Proper function of these organelles depends on two separate genomes, nuclear and mitochondrial. Although the mitochondrial genome (mtDNA) is distinctly smaller than its nuclear counterpart, all mtDNA-encoded proteins are essential for humans (2). The vast majority of mitochondrial proteins are nuclear-encoded and are imported into mitochondria after synthesis in the cytoplasm (3). The mitochondrial proteome comprises over 1500 proteins (3,4); among them are proteins essential for mtDNA replication, transcription, RNA stability and turnover, post-transcriptional modifications and mitochondrial translation (5). The advent of mass-spectrometry-based methods enabled advanced studies of organellar proteomes in different cells, tissues and under various conditions (6–10). Nevertheless, the biochemical function of around 25% of mitochondrial proteins has yet to be defined (11).

The human mitochondrial genome is a circular 16-kb DNA molecule composed of heavy (H-strand) and light (L-strand) strands, which are distinguished by the distribution of guanines and differential sedimentation in ultracentrifugation gradients (12). MtDNA encodes 2 rRNAs, 22 tRNAs and 13 polypeptides, most of which are transcribed from the H-strand. RNA synthesis from the L-strand comprises only one protein-coding gene and 8 tRNAs and results mostly in non-coding antisense RNAs. Transcription of both mtDNA strands is initiated within a non-coding regulatory region (NCR) and spans almost the entire genome (2,12). As a result, polycistronic transcripts are formed that are further processed to produce mature functional RNA molecules (13,14). The mitochondrial transcription machinery appears to be simple, composed of a monomeric RNA polymerase, POLRMT and only a few known co-factors: TFAM, TFB2M and TEFM (2,15). Interestingly, the levels of mitochondrial RNAs are not necessarily correlated with the copy number of mtDNA (16). Moreover, upregulation of mitochondrial transcription precedes replication of mtDNA when cells recover from tran-

*To whom correspondence should be addressed. Tel: +48 22 592 30 23; Fax: +48 22 592 21 90; Email: rszczesny@ibb.waw.pl

sient depletion of the mitochondrial genome (17). While the basics of mitochondrial transcription have been established (15), it is largely unknown how mitochondrial gene expression responds to conditions in which mtDNA copy number is transiently reduced or transcription of mtDNA is hampered by stressors.

Several approaches have been applied to unravel the mechanisms of RNA metabolism in human mitochondria (11,18–21) yet our understanding of mitochondrial gene expression is still far from complete (22). Here we applied quantitative proteomic screening to identify new proteins whose levels are differentially regulated in response to perturbed mitochondrial gene expression. Analysis of the mitochondrial proteomes of human cells deprived of mtDNA has been reported (23); however, this data presents a static picture of mtDNA-depleted cells that have adapted to this situation during many years of culture.

In the present study we examined changes occurring upon transient mtDNA depletion and found the novel mitochondrial regulator C6orf203, which we named MTRES1. Our quantitative proteomic approach showed that MTRES1 is upregulated upon disruption of mitochondrial nucleic acid synthesis. We confirmed the mitochondrial localization of MTRES1 and showed that MTRES1 restores mtRNAs levels in stress conditions. Our data indicates that MTRES1 acts at the transcriptional level without influencing the stability of mitochondrial transcripts. The protective function of MTRES1 stems from its RNA-binding activity, which identifies this protein as a novel validated mitochondrial RBP. We report that MTRES1 is important for the transcriptomic output of the NCR of mtDNA and propose that upregulation of MTRES1 upon inhibition of mitochondrial nucleic acid synthesis acts as a compensatory mechanism to rescue diminished mitochondrial transcription.

MATERIALS AND METHODS

Cell lines, cell culture and DNA cloning

Cells were cultured in Dulbecco's-modified Eagle's medium (DMEM) medium (Gibco) supplemented with 10% FBS (Gibco) at 37°C under 5% CO_2. Expression of the transgenes was induced with tetracycline (100 ng/ml). The 293 Flp-In T-REx cells (R78007, Thermo Fisher Scientific) or derivative stably transfected cell lines were used. Stable cell lines were obtained as previously described (24). DNA cloning was performed with the help of sequence and ligation independent strategy using procedures which we described in details elsewhere (24). All DNA constructs used for establishing stable cell lines are listed in Supplementary Table S2.

BrU labeling and single-cell resolution fluorescence microscopy

Cells were plated on 384-well microplates (781946, Greiner, Bio-One) and expression of the transgene was induced with tetracycline (100 ng/ml) for 48 h before treatment with transcription inhibitors. Cell seeding as well as further manipulations were performed with the use of the Multidrop Combi Reagent Dispenser (Thermo Fisher Scientific). Wash steps were performed with the 405 LS Microplate Washer (Bio Tek). Transcription inhibitors were added to the medium (time and concentration of the reagents as indicated on Figure 4D and E) and after the indicated incubation time 5-Bromouridine solution (Sigma, final concentration of 2.5 mM), containing (or not) inhibitors diluted to their final concentration in the well, was added for 1 h. Inhibitors treatment as well as BrU labeling was performed at 37°C under 5% CO_2. Cells were then fixed by the addition of the fixing solution to the final concentration: 5% (v/v) formaldehyde, 0.25% (w/v) Triton X-100, 2 ng/ml Hoechst 33342 in phosphate-buffered saline (PBS) for 30 min at room temperature followed by washing four times with PBS and blocking (3% (w/v) bovine serum albumin in PBS) for 30 min. Cells were incubated overnight at 4°C with anti-BrdU antibodies (ab6326, Abcam) diluted 1:600 with the blocking solution. Cells were washed four times with PBS and secondary antibodies conjugated with Alexa Fluor 555 at 1:800 in the blocking solution were applied for 1 h followed by washing with PBS. Cells were kept in PBS for imaging. Data were collected using ScanR fluorescence microscopy system (Olympus, UPlanSApo 20.0× objective). Image analysis was performed using ScanR 2.7.2 analysis software (Olympus). Mitochondrial transcription was quantified. This was achieved by staining cells with Hoechst 33342 to stain nuclei, determine their position and area within the cell. Moreover, mitochondria were stained to control co-localization of BrU-labeled RNAs with these organelles. In post-imaging data analysis virtual channels were created for BrU and nuclei, and background was subtracted. An object mask was created for the nuclei and it was excluded for the BrU spots quantification. Mean fluorescent intensity of remaining (mitochondria-overlapping) BrU-spots per cell was calculated.

Mitochondria isolation

Mitochondria isolation was performed as described previously (25) with minor modifications. Cells were centrifuged at 400 × *g* for 8 min at 4°C after harvesting from the plate in NKM buffer (1 mM Tris–HCl, pH 7.4, 0.13 M NaCl, 5 mM KCl, 7.5 mM $MgCl_2$). Following centrifugation and resuspention of the pellet in ice-cold homogenization buffer (4 mM Tris-HCl, pH 7.8, 2.5 mM NaCl, 0.5 mM $MgCl_2$) ten strokes of a tight-fitting pestle (Dounce homogenizer) were applied to homogenize the cells. Nuclei and cell debris were pelleted by two centrifugations at 900 × *g* for 4 min at 4°C. Mitochondria were pelleted by centrifugation at 10 000 × *g* for 2 min at 4°C. In case of the highly purified mitochondria preparation, the following steps were performed: mitochondrial pellet was resuspended in H buffer (225 mM mannitol, 75 mM sucrose, 10 mM HEPES-NaOH pH 7.8, 10 mM ethylenediaminetetraacetic acid (EDTA)) and centrifuged at 10 000 × *g* for 2 min at 4°C. Pellets were resuspended in H buffer and ultracentrifugation in 1M/1.5M sucrose gradient was performed at 45 000 × *g* for 1 h at 4°C (WH ultracentrifuge Sorvall ThermoFisher Scientific, TH-641 rotor). Purified mitochondria were collected from the interphase, washed twice with H buffer and pelleted by centrifugation at 10 000 × *g* for 2 min at 4°C.

Mitoplasts preparation

Isolated mitochondria were resuspended in HomB buffer (40 mM Tris–HCl pH 7.6, 25 mM NaCl, 5 mM MgCl2) and lysed with 1% Triton X-100 or incubated with 0.1% Digitonin (D5628, Sigma) for 10 min on ice. Afterward, samples were centrifuged at 7000 × *g* for 2.5 min at 4°C. Pellets were resuspended in HomB buffer with or without 0.1 mg/ml Proteinase K (EO0491, ThermoFisher Scientific) followed by incubation on ice for 20 min. Proteinase K-treated samples were centrifuged at 7000 × *g* for 2.5 min at 4°C and pellets were resuspended in HomB buffer supplemented with 2 mM PMSF to inhibit proteinase K. Intact mitochondria and mitoplasts were pelleted and lysed in HomB buffer supplemented with 1% Triton X-100, 2 mM PMSF and a protease inhibitor cocktail (Roche). Equal amounts of each lysate were subjected to western blot analysis.

EtBr treatment and mass spectrometry

Cells were cultured in DMEM medium (Gibco) supplemented with 10% FBS (Gibco), 1 mM sodium pyruvate (Sigma) and 50 μg/μl uridine (Sigma) and treated (or not) with ethidium bromide (100 ng/ml) for 72 h. Afterward highly purified mitochondria were isolated as described in the 'mitochondria isolation' paragraph. Lysis buffer (25 mM HEPES, 2% sodium dodecyl sulphate, protease and phosphatase inhibitors) was added to the isolated mitochondria. Samples were heated at 96°C for 3 min, cooled down, sonicated (20 cycles: 30 s on/30 s off) and heated again for 3 min at 96°C. Protein concentration was determined using DirectDetect Spectrometer (MerckMillipore). Appropriate volumes containing accordingly 75 μg of protein were moved to 1.5 ml tubes and precipitated using the chloroform/methanol protocol (26): proteins were mixed with four volumes of methanol, briefly vortexed and mixed with one volume of chloroform, after which samples were briefly vortexed and three volumes of water were added. After vortexing samples were centrifuged for 2 min at 14 000 × *g* at 22°C. The aqueous phase was discarded and four volumes of methanol were added. Samples were briefly vortexed and centrifuged for 3 min at 14 000 × *g* at 22°C. The supernatant was discarded and the pellet was dried at room temperature. Samples were then labeled using the standard iTRAQ 8-plex (SCIEX) protocol according to manufacturer recommendations. Labeled peptide mixture was speed-vaced to dry and then dissolved in 400 μl of a buffer containing 30% acetonitrile (ACN) and 0.1% trifluoroacetic acid (TFA). Solution was pre-separated on a Superdex Peptide 10/300 GL column, 30 min long isocratic gradient of 30% ACN 0.1% TFA, flow 0.6 ml/min, fractions were collected at 800 μl each. Three consecutive fractions were pooled into one and speed-vaced to dry. MS analysis was performed by LC-MS in the Laboratory of Mass Spectrometry (IBB PAS, Warsaw) using a nanoAcquity UPLC system (Waters) coupled to an LTQ-Orbitrap QExactive mass spectrometer (Thermo Fisher Scientific). The mass spectrometer was operated in the data-dependent MS2 mode, and data were acquired in the m/z range of 100–2000. Peptides were separated by a 300 min linear gradient of 95% solution A (0.1% formic acid in water) to 45% solution B (ACN and 0.1% formic acid). The measurement of each sample was preceded by three washing runs to avoid cross-contamination. Obtained data were analyzed with the MaxQuant platform. The human reference proteome database from UniProt was used. The following modifications were set: oxidation(M), methylthio(C). Results were analyzed using the Scaffold 4 platform (Proteome Software).

RNA isolation and northern blot

RNA was isolated with the use of TRI Reagent according to the manufacturer's instructions. Northern blot was performed according to standard protocol described elsewhere (25). Shortly, 1 μg of RNA was run on an agarose gel followed by overnight capillary transfer to Hybond-N membrane (GE Healthcare). DecaLabel DNA Labeling Kit (Thermo Fisher Scientific) was used to radioactively label probes with [α-32P] dATP (Hartmann Analytic). In case of strand-specific hybridizations (Figure 5), *in vitro* transcription was performed utilizing polymerase chain reaction (PCR) products containing S6 or T7 promoter sequence (one on each end) as a template. Primers used to generate PCR products applied as templates for obtaining radiolabeled probes are listed in Supplementary Table S3. Results were recorded after overnight exposure to PhosphorImager screens (FujiFilm) using Typhoon FLA 9000 scanner (GE Healthcare). Quantification was performed using Multi Gauge V3.0 software (Fujifilm).

Western blot

Protein extracts were prepared and processed as previously described (25). Primary antibodies used in this work are listed is Supplementary Table S4. Appropriate secondary antibodies conjugated with horseradish peroxidase were applied diluted 1:10 000 (401393, 401215, Calbiochem and A5420, Sigma).

Immunoprecipitation

For immunoprecipitation (IP), 293 parental cells and cell lines stably expressing mitochondrially targeted EGFP (mitoEGFP) and C-terminally EGFP-tagged MTRES1 (MTRES1-EGFP) were used. In both stable cell lines EGFP sequence is preceded with TEV protease recognition site (mito-TEV-EGFP, MTRES1-TEV-EGFP) thus the tag can be cleaved off by TEV treatment releasing rest of the fusion protein. This approach is described in detail in Szczesny *et al.* (24). Expression of the transgenes was induced with tetracycline (100 ng/ml) for 48 h before treatment with EtBr. Cells were treated (or not) with EtBr (100 ng/ml) for 24 h. Afterward, mitochondria were isolated as described in 'mitochondria isolation' section. Lysis buffer (50 mM Tris–HCl pH 8.0, 100 mM NaCl, 1% Triton X-100 (v/v) supplemented with protease and phosphatase inhibitors) was added to the isolated mitochondria. Samples were incubated with rotation at 4°C for 10 min followed by sonication (20 cycles: 15 s on/45 s off) and centrifugation for 10 min at 12 000 × *g* at 4°C. For RNase A treatment, samples were divided into two equal fractions before sonication and one fraction was supplemented with RNase A (Sigma) to final concentration of 20 μg/ml. Supernatant was collected and magnetic affinity beads (GFP-Trap, Chromotek)

were added followed by incubation with rotation at 4°C for 60 min. Beads were collected on the magnetic stand and washed three times with wash buffer (50 mM Tris–HCl pH 8.0, 100 mM NaCl). Elution was performed by addition of TEV protease in TEV buffer (50 mM Tris–HCl pH 8.0, 150 mM NaCl, 0.1% Triton X-100 (v/v)) and incubated for 90 min at room temperature. Elution was collected by discarding beads on the magnetic stand.

DSP crosslinking

DSP (dithiobis[succinimidylpropionate], Thermo Fisher Scientific) was dissolved in DMSO (dimethyl sulfoxide, Sigma) shortly before the experiments were carried out. Cells were harvested and suspended in PBS followed by the addition of DSP to final concentration of 0.5 mM. Cells were incubated with rotation at 4°C for 30 min. Crosslinking was quenched by addition of Tris–HCl pH 7.4 to 50 mM and incubation with rotation at 4°C for 15 min. Then, samples were centrifuged at 700 × *g* at 4°C followed by mitochondria isolation and IP as described in the 'IP' paragraph.

In vitro transcription and radiolabeling

In vitro transcription was performed with the use of T7 Transcription Kit (ThermoScientific) according to manufacturer's instructions with the addition of [α-32P] UTP (Hartmann Analytic). As a template for *in vitro* transcription, PCR products containing SP6 or T7 promoter sequence (one on each end) were used. Primers used in the study are listed in Supplementary Table S3. DNA template was removed by DNase I digestion and obtained radiolabeled transcripts were purified on the spin columns with the use of Sephadex G-50 gel filtration medium (GE Healthcare).

Library preparation and next-generation sequencing

RNA-seq experiment was performed in triplicate according to the protocol described previously (24) except for the use of a Ribo-Zero rRNA Removal Kit (Human/Mouse/Rat, Illumina) for rRNA removal and the use of CutSmart buffer (New England BioLabs) for digestion with USER Enzyme (New England BioLabs). Sequencing was carried out on an Illumina NextSeq 500 sequencing platform, using a NextSeq 500 High Output Kit (150 cycles) (FC-404-1002, Illumina) and pair-end sequencing procedures of 2 × 75 cycles (Instructions: 15048776 Rev. D, 15046563 Rev. F).

Analysis of next-generation sequencing data

RNAseq raw data were preprocessed with FastQC v 0.11.3 and trimmed of adapters using cutadapt v 1.9.2.dev0. Low-quality bases and improperly paired reads were removed prior to mapping using Trimmomatic v 0.32. Trimmed reads were mapped to the human genome (GRCh38) using the STAR aligner v 2.5.2b with soft-clipping allowed (default type of alignment) and the basic GENECODE v26 annotation with introduced features that allowed for the quantification of all reads mapped in the D-loop region. Mapped reads were counted using htseq-count v 0.9.1 and normalized in the edgeR package v 3.18.1. Wiggle files of uniquely mapped reads were converted to the BigWig format with the use of wigToBigWig package. Tracks of mapped reads were displayed using the Integrative Genomics Viewer (IGV) and, for the purpose of preparing a figure, assembled using graphical software (CorelDraw). Gene silencing efficiency was examined by calculating the ratio of MTRES1 gene expression fold change in reference to the parental 293 sample and by visual inspection of IGV gene track against the adequate MTRES1 variant (Transcript ID ENST00000311381.7, RefSeq NM_016487).

Conserved domain search, sequence alignment and structure representation

Conserved domain search was performed with the use of the CD-Search tool (27). Protein sequence alignment was performed with the use of Clustal 2.1 program (28). Structure representation was prepared using PyMOL software.

Protein purification

MTRES1 (86–240 aa, UniProt ID: Q9P0P8) was expressed as a C-terminal 6xHis fusion protein. N-terminal truncation was designed according to Edman sequencing results indicating the mature form of MTRES1 protein. Point mutations (R143A, D145A, K149A, R156A, K157A) were introduced using a standard site-directed mutagenesis approach. An *E. coli* BL21 strain was transformed with plasmids listed in Supplementary Table S2 for protein expression. Bacteria were cultured for 48 h at 18°C in an auto induction Super Broth Base (Formedium) supplemented with kanamycin (50 μg/ml). Bacteria were pelleted, homogenized in the EmulsiFlex (Avestin) apparatus and obtained extracts were subjected to purification. As a first step, proteins were purified by Ni affinity chromatography followed by gel filtration. The second round of purification encompassed ion exchange chromatography which was performed with the use of a 6 ml Resource Q column (GE Healthcare). Both steps were performed with the use of the ÄKTA express apparatus.

Electrophoretic mobility shift assay

Radiolabeled RNA substrate was prepared as described in the '*In vitro* transcription and radiolabeling' section. Obtained substrates were purified by polyacrylamide gel electrophoresis. EMSA assays were performed using radioactive-labeled RNA at a constant concentration of 10 nM and increasing protein concentrations (up to 5 μM). Binding was performed for 30 min at 30°C in 20 μl reaction volumes containing 10 mM Tris–HCl pH 8.0, 2.5 mM KCl, 50 mM NaCl, 1 mM EDTA, 0.5 mM dithiothreitol (DTT), 1% glycerol and 0.025% Tween-20. Afterward, 4 μl of Loading Dye (10 mM Tris–HCl pH 7.6, 0.03% bromophenol blue, 0.03% xylene cyanol FF, 60% glycerol, 60 mM EDTA) were added (R0611, Thermo Fisher Scientific) and samples were separated in 5% polyacrylamide gel (19:1) at constant 13 W in TBE buffer (90 mM Tris, 90 mM boric acid, 2 mM EDTA). Results were recorded using the Typhoon FLA 9000 scanner (GE Healthcare) after overnight exposure to

the Phosphorimager screens. Quantification was performed using Multi Gauge software (Fujifilm).

DNA isolation and qPCR

Total DNA was isolated following a phenol–chloroform extraction protocol as described previously (29). qPCR was performed with the use of SYBR Green reagents (Roche) according to manufacturer's instructions. Isolated DNA was diluted and 4 ng were used as a template in qPCR reactions. RSZ818 and RSZ819 starters were used to amplify the ND1 gene, relative abundance of ND1 was normalized to nuclear B2M gene fragment amplified with RSZ816 and RSZ817 primers. Primers used for qPCR are listed in Supplementary Table S3.

Data visualization

Graphs were prepared with the use of GraphPad Prism version 6.00 for Windows, GraphPad Software, La Jolla, CA, USA. Bar charts with indicated individual values presented on Figures 3 and 4 were produced using PointBar tool (30).

RESULTS

A quantitative proteomic screen reveals proteome changes upon mtDNA/mtRNA depletion

To search for proteins regulating mitochondrial nucleic acids in response to perturbed mitochondrial gene expression we implemented a quantitative proteomic screen. Our experimental strategy was based on the observation that the level of some proteins engaged in mitochondrial nucleic acids metabolism, including LRPPRC, SLIRP, GRSF1 and TFAM, depends on the mtDNA/mtRNA content (17,31–33) (Figure 1A). We assumed that other proteins, potentially new mtRNA/mtDNA players, may also exhibit this feature (Supplementary Figure S1A). To identify such proteins we analyzed proteomes of highly purified mitochondria from human cells with transiently reduced mitochondrial nucleic acids content using isobaric tag-based quantification coupled with mass spectrometry (Figure 1B). We implemented the iTRAQ method (isobaric Tags for Relative and Absolute Quantification) as it enables reliable quantitative comparison of multiple samples (34). We treated cells with ethidium bromide (EtBr), a well-established mitochondrial DNA replication/transcription inhibitor (17), to induce a pause in mitochondrial nucleic acid synthesis. Because diminished mitochondrial gene expression might result in disturbances of mitochondrial protein import by affecting the potential of the inner membrane, we established a cellular model based on human 293 Flp-In T-REx cells to examine this possibility. We generated a stable 293 cell line that expresses a fusion of EGFP with a mitochondria targeting sequence derived from Cox8a protein under the control of a tetracycline-inducible promoter. Fluorescent microscopy confirmed the mitochondrial localization of the fusion protein (Supplementary Figure S1B), indicating that the protein can be used as a marker for mitochondrial import.

To perform the screen, 293 cells expressing mitoEGFP were treated for 3 days with EtBr and then we harvested the cells and isolated the mitochondria. Isolated organelles were lysed and protein extracts were subjected to iTRAQ-based quantification (Figure 1B). Analyses of mtDNA as well as mitochondrial transcripts levels confirmed their depletion in EtBr-treated cells (Figure 1C and D). Using mass spectrometry we identified 1381 proteins that were common for all samples analyzed (Supplementary Table S1). The extent of mitochondrial proteome coverage observed by us was similar to ones achieved by others (35), covering almost 60% of proteins listed in MitoCarta 2.0, which encompasses predicted and experimentally validated mitochondrial proteins (4) (Figure 1E). We identified over 90% of mitochondrial ribosome components (Supplementary Table S1), suggesting a bias toward highly abundant proteins, an expected feature for mass spectrometry based approaches (36). To identify proteins whose levels depend on mtDNA/mtRNA, we calculated the ratio of the abundance of proteins in EtBr-treated versus untreated cells. Importantly, we found that mitochondrial proteins (MitoCarta 2.0) were overrepresented among downregulated proteins as well as they were present in upregulated proteins (Figure 1F).

In our screen, we expected to observe a decrease in mitochondrially-encoded proteins as well as reference proteins that were described in the literature (17,32–33), which we tested by western blot (Figure 1A). Relative changes observed for these proteins guided us to set the threshold during mass spectrometry data analysis (Figure 1G). Accordingly, we identified 104 proteins as significantly downregulated and 114 proteins as significantly upregulated (Figure 1G).

Gene ontology analysis of proteins whose level was reduced upon mitochondrial nucleic acid depletion showed a significant enrichment of proteins engaged in mitochondria-related processes such as oxidative phosphorylation, respiratory electron transport chain as well as translation (Figure 1H). Indeed, we found depletion of mitochondrial ribosomal proteins as well as mitochondrial and nuclear-encoded subunits of the electron transport chain (Supplementary Table S1) upon EtBr treatment. Notably, we did not observe changes in the level of either mitoEGFP or HSP60 (Figure 1G). Altogether, analysis of down-regulated proteins indicated expected changes in the mitochondrial proteome, validating our experimental approach.

Within the group of proteins which were significantly upregulated, we found proteins responsible for mitochondrial fission/fusion processes as well as redox state regulators (Supplementary Table S1). Interestingly we identified the EXOG protein engaged in mtDNA repair (37) and the mitochondrial DNA polymerase accessory subunit POLG2, which is important for mtDNA maintenance (38) (Figure 1G). Upregulation of POLG2 and EXOG alongside the enrichment of proteins involved in RNA and protein transport and localization (Figure 1I) suggested a possible trigger of a compensatory mechanism(s) in response to disturbed mitochondrial gene expression. Notably, among upregulated proteins we identified proteins of unknown function in mtRNA/mtDNA metabolism. We selected four poorly characterized proteins C16orf58, METTL7A, CEBPZOS,

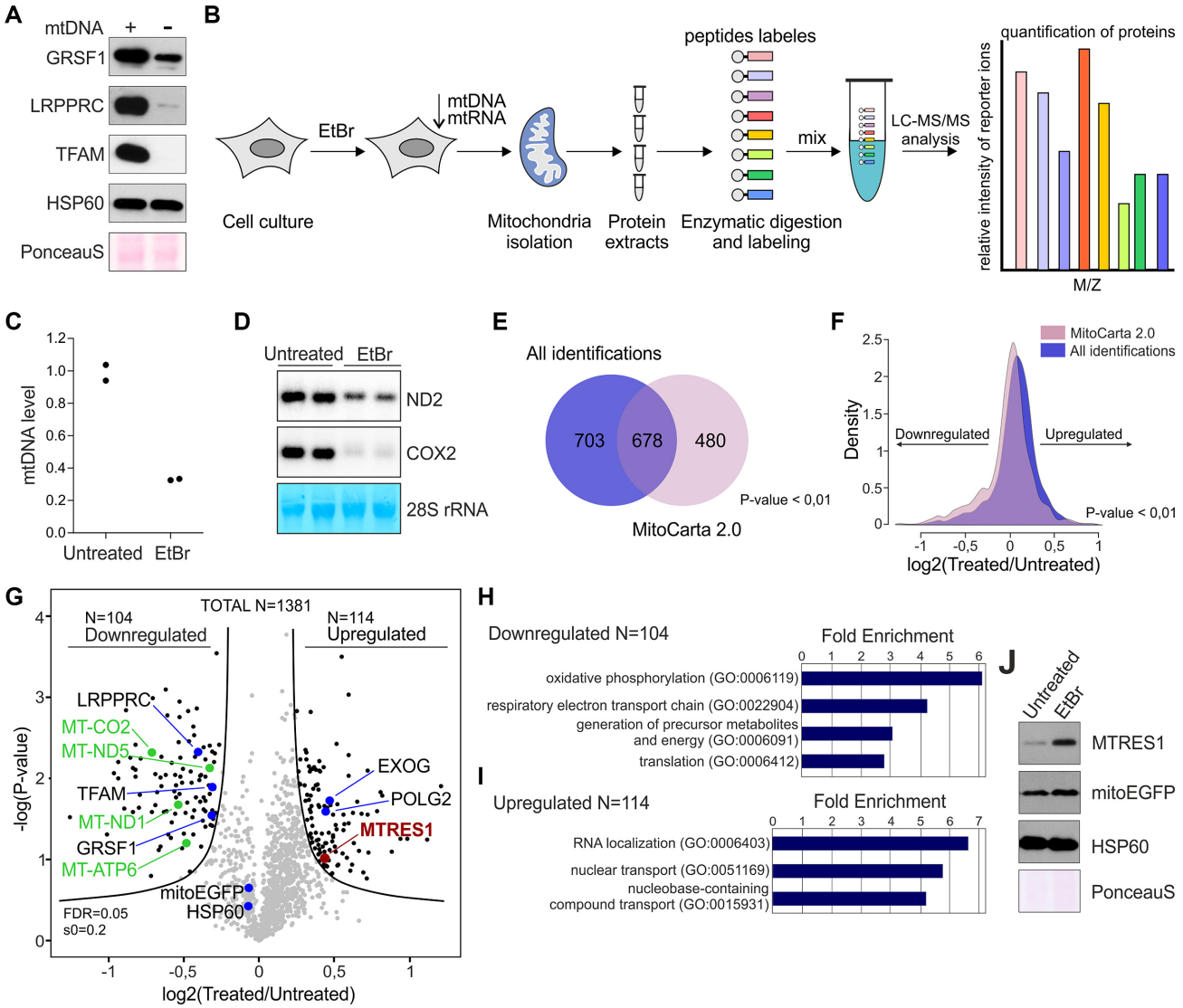

Figure 1. Depletion of mitochondrial nucleic acids changes the mitochondrial proteome. (**A**) Western blot analysis of known mtRNA/mtDNA factors. Protein lysates obtained from A549 cells with normal mtDNA content as well as cells lacking mitochondrial DNA (rho0) were analyzed. PonceauS serves as a loading control. HSP60 represents a mitochondrial protein whose level is independent from mitochondrial nucleic acid content. (**B**) Schematic representation of the experimental workflow. Cells were treated with ethidium bromide (EtBr) to induce mitochondrial nucleic acid depletion. Proteins were extracted from mitochondria and subjected to iTRAQ labeling. Mixed labeled peptides were analyzed by liquid chromatography tandem mass spectrometry. (**C** and **D**) Before mitochondria isolation, a fraction of EtBr-treated and untreated cells was collected for total DNA and RNA isolation. mtDNA level was measured by qPCR (C) whereas mitochondrial transcripts were analyzed by northern blot (D). Results for individual experiments are shown. (**E**) Venn diagram showing overlap between all proteins identified in the course of iTRAQ experiment and proteins present in human MitoCarta 2.0. Statistical significance of the overlap is presented. (**F**) Density plot visualizing distribution of proteins identified and quantified in iTRAQ experiment in reference to their relative abundance changes (treated/untreated). Kolmogorow–Smirnov test was applied to test equality of the distributions. Statistical significance is presented. (**G**) Volcano plot of the proteins quantified in the course of the iTRAQ experiment. Each point represents a protein, protein's fold change in abundance is plotted against statistical significance (*P*-value). Continuous line determines proteins whose expression was significantly altered with FDR < 0.05 and fold-change s0 > 0.2. Proteins mentioned in the text are colored blue. Mitochondrially encoded proteins are colored green. (**H** and **I**) GO analysis of significantly down- (H) an up- (I) regulated proteins. Biological process terms enriched in this group of identifications are ranked based on fold change with FDR < 0.05. (**J**) Confirmation of iTRAQ results with western blot analysis. Lysates of untreated and treated (EtBr) cells were analyzed. Image shows representative result of three replicates. PonceauS staining serves as a loading control.

C6orf203 (renamed MTRES1) for bioinformatic analysis of conserved domains and subcellular localization prediction. As a result, we focused on the MTRES1 protein. Importantly, an increased level of this protein upon EtBr treatment was independently confirmed by western blot analysis of protein lysates from three additional independent experiments (Figure 1J), which prompted us to study MTRES1 further as a potential factor engaged in response to perturbed mitochondrial gene expression.

MTRES1 is a novel mitochondrial RNA-binding protein

Our proteomic analysis of purified mitochondria suggested that MTRES1 is a mitochondrial protein, a conclusion further strengthened by the fluorescence microscopy analysis of 293 cells expressing MTRES1-EGFP (Figure 2A). This analysis showed that the fluorescent MTRES1-EGFP fusion colocalizes with a mitochondria-specific dye (Figure 2A). To see if MTRES1 can be directly involved in the mtRNA/mtDNA metabolism we tested if the protein is localized in the mitochondrial matrix, where mitochondrial nucleic acids transactions take place. To study the submitochondrial localization of the endogenous MTRES1, we isolated mitochondria from 293 cells, prepared mitoplasts by removing the mitochondrial outer membrane with digitonin and subjected them (or not) to proteinase K treatment (Figure 2B). As a marker of successful mitoplast preparation we monitored the integrity of the mitochondrial inner membrane protein OXA1L whose N-terminal part is exposed to the intermembrane space, thus being susceptible to proteinase K degradation upon outer membrane disruption (39). While OXA1L was highly degraded by proteinase K in digitonin-treated mitochondria, a known mitochondrial matrix protein LRPPRC (40) remained intact, similarly to MTRES1 (Figure 2B). This led us to the conclusion that MTRES1 is a mitochondrial matrix protein.

A sequence search of MTRES1 against the Conserved Domain Database (27) suggested the presence of an S4 RNA-binding domain (Figure 2C). In bacteria S4 proteins play an important role in ribosome biogenesis where they initiate ribosome assembly by organizing rRNA structure and enabling successive ribosomal proteins to bind rRNA (41). In human cells, S4 protein is a constituent of the cytoplasmic small ribosome subunit but is postulated to be absent from the mammalian mitochondrial ribosome (42–44). In line with these findings, we did not observe co-IP of mitochondrial ribosome proteins with MTRES1-EGFP (Supplementary Figure S2). Nevertheless, it was possible that MTRES1 has another function that involves putative RNA-binding ability.

Therefore, we sought to investigate if MTRES1 is able to bind RNA. We performed *in vivo* crosslinking and IP with the use of an established stable cell line expressing EGFP-tagged MTRES1 (45), which indicated that MTRES1 binds RNA *in vivo* (Supplementary Figure S3A and B). IP of MTRES1-EGFP and analysis of co-precipitated RNAs with the use of qPCR showed that MTRES1 binds a broad spectrum of mitochondrial transcripts without pronounced preference as compared to the well-established mitochondrial RNA-binding protein LRPPRC (Supplementary Figure S3C and D). To confirm a direct interaction of MTRES1 with RNA, we purified the protein after heterologous expression. To be able to do so, we first established the N-terminus of the mature MTRES1 since most mitochondrial matrix proteins undergo N-terminal proteolytic processing after import into mitochondria (46). Because *in silico* analysis of the MTRES1 sequence was insufficient to unambiguously determine the processing site of the protein (Supplementary Figure S4A), we purified MTRES1 from mitochondria isolated from 293 cells and subjected it to sequencing by Edman degradation. This approach revealed that the mature protein is shorter by 84 amino acids on the N-terminus (Figure 2C and Supplementary Figure S4A-B). Therefore, MTRES1 devoid of the N-terminal 84 amino acids was expressed in bacteria and purified by affinity chromatography (Figure 2D). Multiangle light scattering (MALS) indicated that the mass of the purified protein was very similar to its theoretical mass (19.36 kDa versus 18.25 kDa), showing that the protein is a monomer. To see if MTRES1 binds RNA directly, we performed an electrophoretic mobility shift assay using *in vitro* transcribed radiolabeled mitochondrial 7S RNA as a substrate and observed that MTRES1 was able to bind the substrate (Figure 2E). Thus, we concluded that MTRES1 is a mitochondrial matrix RNA-binding protein that exists in a monomeric form.

Silencing of MTRES1 affects RNAs originating from the non-coding regulatory region

The RNA-binding ability of MTRES1 suggested that the protein may be involved in mtRNA metabolism. Therefore, we examined the effect of MTRES1 depletion on the mitochondrial transcriptome using a cellular model that enables tetracycline-inducible miRNA silencing of the gene in question (Supplementary Figure S5), an approach which we applied previously to study other proteins (47,24). We obtained two stable cell lines derived from human 293 Flp-In T-Rex cells; one cell line inducibly expresses miRNAs silencing the endogenous copy of MTRES1 gene (hereafter MTRES1 silencing), while the second cell line expresses FLAG-tagged MTRES1 containing silent mutations that cause insensitivity to miRNA (hereafter MTRES1 rescue) in addition to inducibly expressing MTRES1-targeting miRNAs. Consequently, in the former case the MTRES1 protein should be depleted whereas in the latter case the endogenous version of MTRES1 should be depleted and replaced by the MTRES1-FLAG protein. Silencing of the endogenous protein was confirmed by western blot, which showed that MTRES1 was not detectable already after 3 days of induction with tetracycline whereas exogenous MTRES1-FLAG was expressed and was resistant to miRNA (Figure 3A).

To investigate global changes in the mitochondrial transcriptome upon silencing of MTRES1 we performed an RNA-seq analysis (Figure 3B and C). We prepared strand-specific RNA-seq libraries using RNA isolated from parental 293 cells, silencing and rescue MTRES1 cell lines collected 3 days after induction with tetracycline. Silencing of endogenous MTRES1 was confirmed at protein and RNA levels (Figure 3A and Supplementary Figure S6, respectively) and we confirmed that the protein detected in

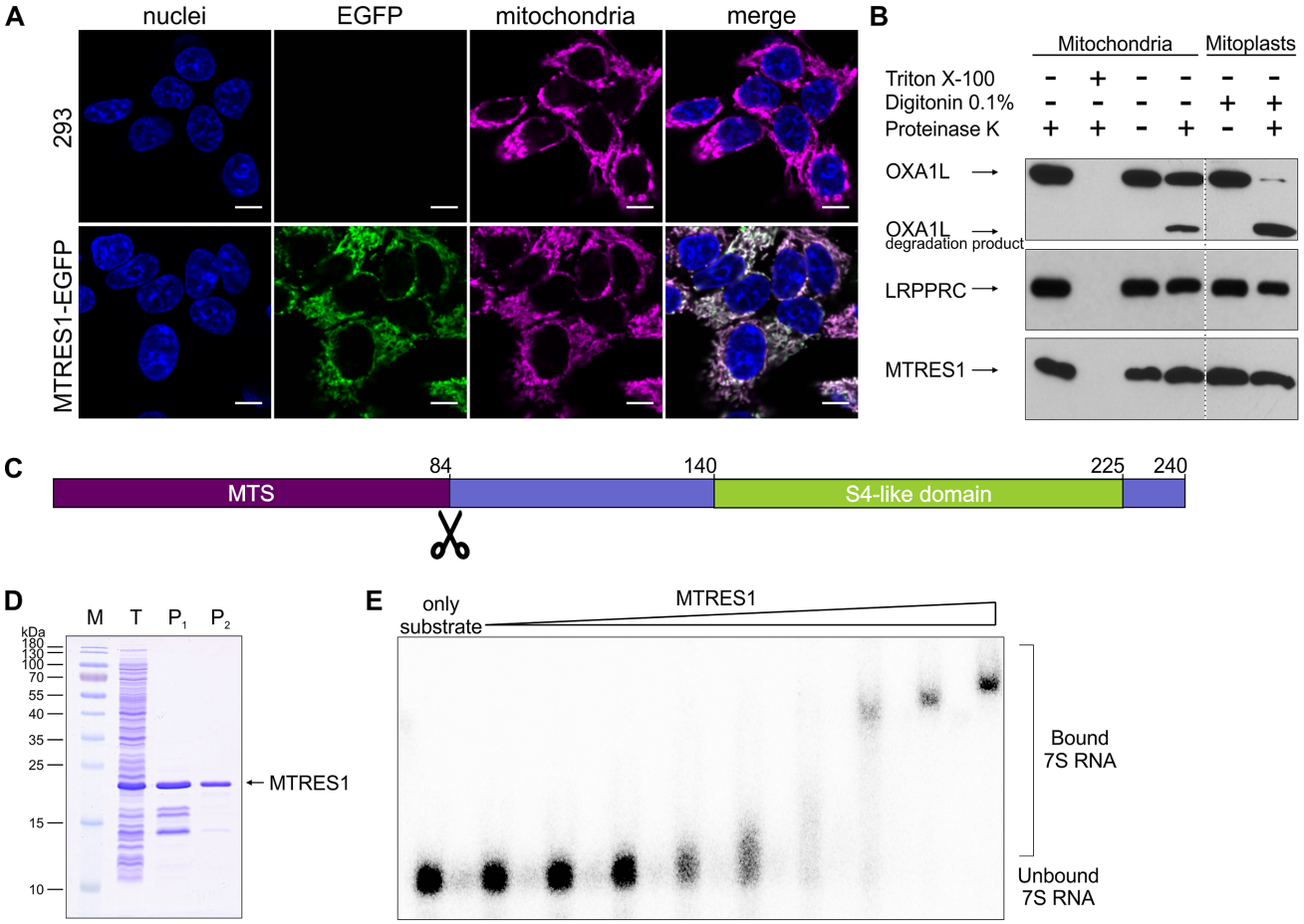

Figure 2. MTRES1 is a mitochondrial RNA-binding protein. (**A**) Intracellular localization studies of MTRES1 tagged with EGFP at the C-terminus. Nuclei and mitochondria were stained with Hoechst and MitoTracker Deep Red, respectively. Confocal microscopy was performed. Merged image shows colocalization of MTRES1 (green) and mitochondria (magenta). Scale bar, 10 μm. (**B**) Western blot analysis of indicated proteins in mitochondria and mitoplasts isolated from 293 cells and treated (or not) with proteinase K. Treatment with Triton X-100 results in disruption of both mitochondrial membranes whereas digitonin disrupts only the outer membrane, increasing degradation of a part of the OXA1L protein exposed to the intermembrane space. LRPPRC serves as a mitochondrial matrix marker. (**C**) Schematic representation of the MTRES1 sequence. Edman degradation indicated the cleavage site of mitochondrial targeting sequence (MTS) (see Supplementary Figure S4 for details). *In silico* analysis of MTRES1 primary structure revealed the presence of an S4-like RNA binding domain. (**D**) Purification of mature MTRES1. Recombinant protein was purified by heterologous expression in bacteria. Protein marker (M), total bacterial lysate (T) and different purification steps (P1, P2) are shown. Highly purified protein (P2) was used to perform all biophysical and biochemical analyses. (**E**) EMSA assay using *in vitro* transcribed 7S RNA substrate and increasing concentrations of purified MTRES1 protein.

MTRES1 rescue cell line resulted from the expression of the ectopic copy of the gene (Supplementary Figure S6B).

RNA-seq analysis, including reads coverage and distribution of reads mapping to mitochondrial genome, indicated that MTRES1 silencing caused a reduction of the 7S RNA level originating from transcription of the NCR while the levels of other mtDNA-encoded transcripts were not altered (Figure 3B and D). Importantly, the effect on NCR-transcribed RNAs was prevented by the expression of a miRNA-insensitive form of MTRES1, confirming that the observed decrease of 7S RNA resulted from MTRES1 silencing and not from miRNA off-targets. Northern blot analysis showed a significant reduction of 7S RNA levels and no effect on other examined mitochondrial transcripts upon MTRES1 silencing, confirming results of RNA-seq (Figure 3E). Moreover, northern blot hybridization showed that expression of miRNA-insensitive MTRES1-FLAG restored 7S RNA levels, in accord with the RNA-seq results (Figure 3E). To see whether MTRES1 regulates 7S RNA levels by influencing the stability of this transcript, we examined if silencing of MTRES1 impacts the degradation rate of 7S RNA. We inhibited mitochondrial transcription and analyzed changes in 7S RNA levels and found the same profile of changes in 7S RNA levels in MTRES1-silenced and control cells (Supplementary Figure S7), indicating that MTRES1 does not contribute to regulation of 7S RNA stability but rather to production of this RNA.

Elevated levels of MTRES1 prevent stress-induced deficiency of mitochondrial transcription

Our analyses revealed that MTRES1 silencing causes a decrease in the LSP-proximal transcript 7S RNA. Interestingly, the 7S RNA level has been suggested to correlate with *de novo* transcription efficiency (48,49). Since we iden-

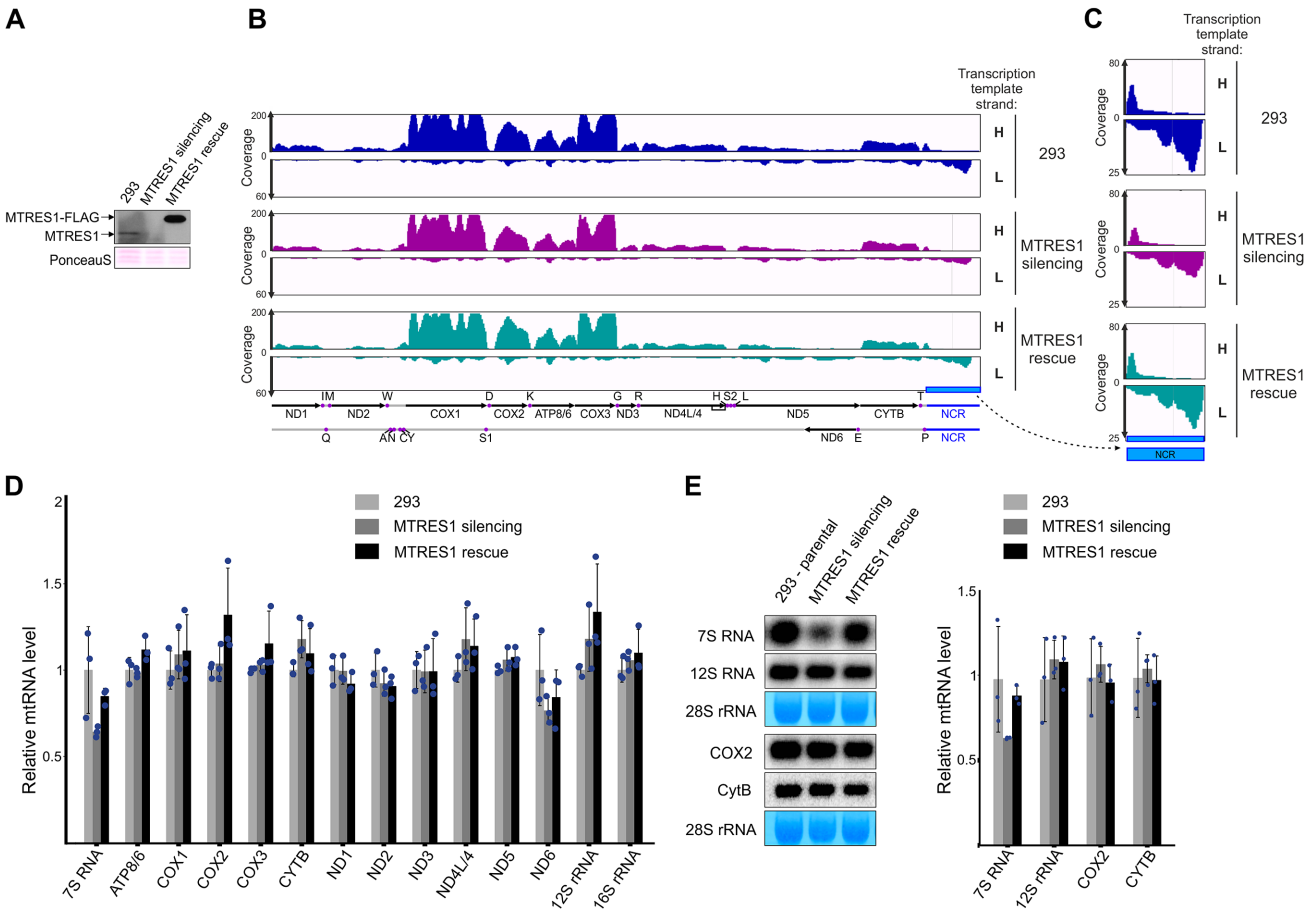

Figure 3. MTRES1 silencing causes downregulation of RNAs originating from the NCR. (**A**) Western blot analysis of parental 293 cells (293), cells with silenced MTRES1 (MTRES1 silencing) as well as cells expressing ectopic version of FLAG-tagged MTRES1 which replaces miRNA-silenced endogenous copy of MTRES1 (MTRES1 rescue). Anti-MTRES1 antibodies were used. Endogenous and FLAG-tagged versions of MTRES1 are indicated with the arrows. PonceauS membrane staining serves as a loading control. (**B** and **C**) Tracks of mapped reads obtained in RNA-seq experiment. Panel C shows zoomed-in NCR region. The experiment was performed in triplicate. A map of mitochondrial transcripts is shown. (**D**) Quantification of normalized RNA-seq counts. mtRNA level relative to 293 parental cells was calculated (mean in 293 was set as 1). Mean (± SD) and individual values are shown. (**E**) Confirmation of RNA-seq results with northern blot hybridization. Methylene blue staining of nuclear-encoded rRNA serves as a loading control. Graph shows quantification of northern blot results. mtRNA level relative to 293 parental cells was calculated (mean in 293 was set as 1). Mean (± SD) and individual values are shown.

tified MTRES1 as a protein increased in response to mitochondrial nucleic acids loss, we asked if upregulation of this protein may serve as a compensatory mechanism to rescue diminished transcription. Using a stable 293 cell line that inducibly upregulates MTRES1 (Figure 4A), we analyzed mtRNAs levels after treatment with EtBr, which mimicked conditions of our initial proteomic screen; however, we applied a shorter EtBr treatment to stall transcription rather than decrease mtDNA levels. We found that upregulation of MTRES1 prevents EtBr-caused decrease of 7S RNA and other tested mtRNAs (Figure 4B). This effect was not caused by altered levels of mitochondrial RNA polymerase POLRMT nor mitochondrial transcription initiation factor TFAM as the levels of these proteins were unaffected by upregulation of MTRES1 (Figure 4A). Importantly, we confirmed that the observed protective role is specific to MTRES1 upregulation as an overexpression of mitochondrially targeted EGFP did not show a similar effect (Supplementary Figure S8). Moreover, analysis of mtDNA levels did not reveal differences between control and MTRES1 upregulating cells treated or not with EtBr (Supplementary Figure S9), indicating that MTRES1 acts at an RNA level and not by increasing mtDNA copy number.

To determine if MTRES1 functions at the transcriptional or post-transcriptional gene expression step we applied two approaches. First, we measured mitochondrial transcription rates under varying stress conditions, and second, we examined decay rates of mitochondrial RNAs to see if RNA degradation may be prevented by MTRES1 upregulation. Moreover, we also checked if the protective role of MTRES1 on mtRNA levels is EtBr-specific or is linked to a general response to mitochondrial transcriptional stress by treating cells with low levels of three different transcription inhibitors: actinomycin D (ActD), 3′-deoxyadenosine (Cordycepin) and EtBr. While ActD and EtBr are postulated to inhibit transcription by intercalation to nucleic acids and interfering with transcription machinery, Cordycepin acts as a chain terminator. Thus it has clearly a different mode of action than the two other inhibitors. Importantly, all three have been used to study

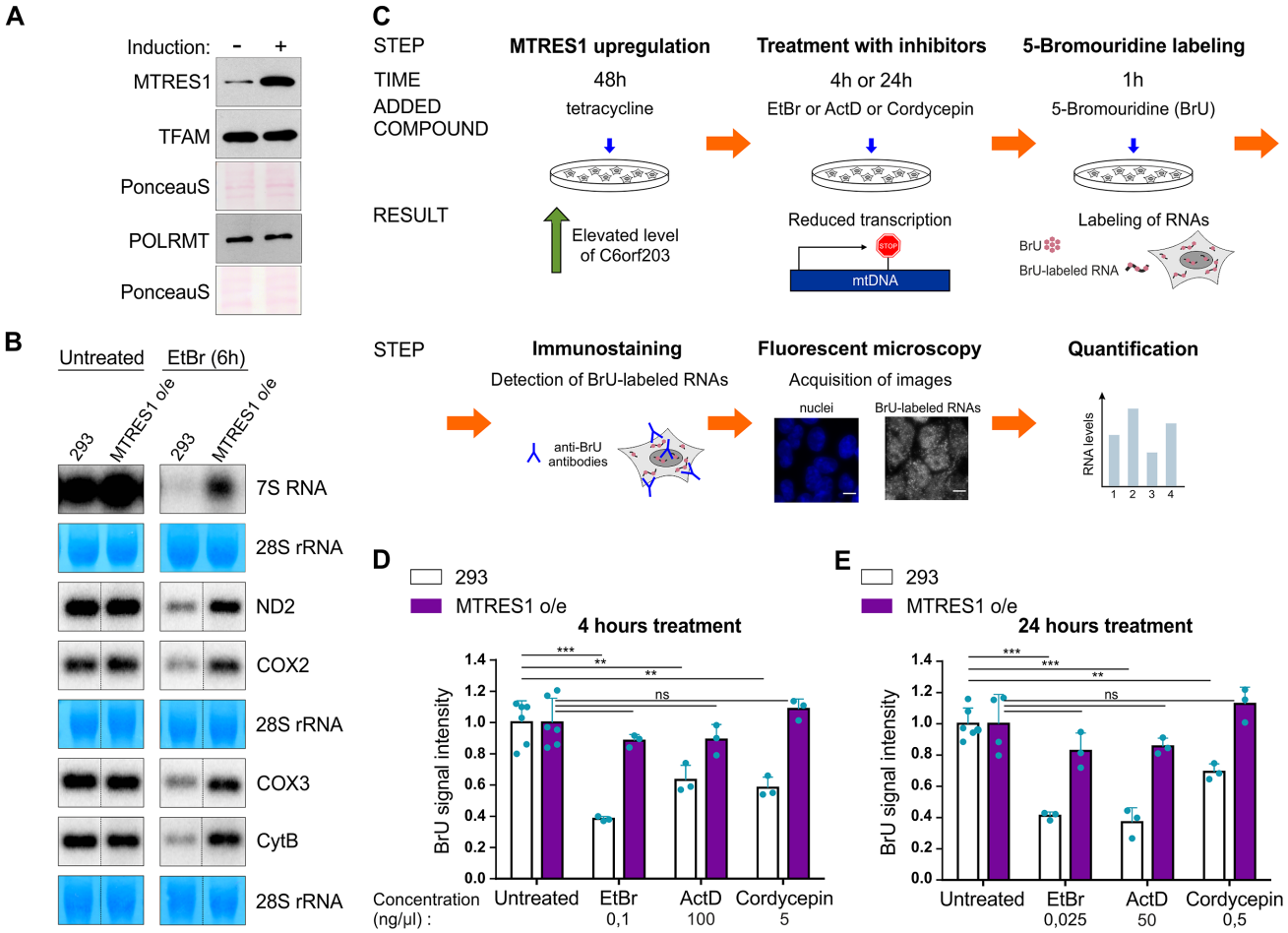

Figure 4. MTRES1 prevents mtRNAs deficiency caused by stalled mitochondrial transcription. (**A**) Western blot analysis of MTRES1, TFAM and POLRMT levels. Specific antibodies were used to detect each protein. PonceauS membrane staining serves as a loading control. (**B**) Northern blot analysis of indicated mtRNAs. RNA isolated from parental 293 cells (293) or cells overexpressing MTRES1 (MTRES1 o/e) treated (or not) with EtBr was analyzed. Methylene blue staining of nuclear-encoded rRNA serves as a loading control. (**C**) Schematic representation of single-cell resolution fluorescence microscopy approach. (**D** and **E**) Quantification of single-cell resolution fluorescence microscopy data. Mean intensity of mitochondrial BrU signal corresponding to nascent transcription events was calculated. Cells were treated for 4 (D) or 24 (E) h with indicated inhibitors. Individual values from the replicates are shown where in each replicate $n > 500$ cells (D) or $n > 250$ cells (E) were analyzed. Graphs show mean from the replicates ± SD. A two-tailed unpaired *t*-test was applied (**$P < 0.001$, ***$P < 0.0001$).

mtRNA turnover (50–52). Using those inhibitors enabled us to examine whether MTRES1 upregulation would prevent mtRNAs loss during different kinds of transcription stress. We used 293 parental control cells and the stable 293 cell line inducibly upregulating MTRES1. Cells were seeded in a 384-well format and after 48 h of MTRES1 expression induction, transcription inhibitors were added to the medium. After 4 or 24 h of treatment nascent transcripts were labeled *in vivo* with bromouridine (BrU). Cells were then fixed and BrU-labeled RNAs were detected with the use of anti-BrU antibodies. We collected images by high-throughput fluorescence microscopy and quantitatively analyzed signals arising from nascent transcripts with a single cell resolution (Figure 4C). Importantly, our post-imaging data analysis allowed us to restrict the quantitative analysis to mitochondrial transcription. We found that upregulation of MTRES1 prevents transcript loss in inhibitor-treated cells as we observed higher quantified intensities of mitochondrial BrU-labeled RNAs in cells overexpressing MTRES1 in comparison to parental cells (Figure 4D and E). Markedly, we observed the same effect independently from the transcription inhibitor used.

To examine decay rates of mitochondrial RNAs, we shut-off mitochondrial transcription completely by the addition of high ActD concentration (5µg/µl) and analyzed the decrease of selected L- and H- strand mitochondrial transcripts by northern blot (Figure 5A). The stability of analyzed mtRNAs was the same in all samples (Figure 5B), indicating that the protective function of MTRES1 is not connected with post-transcriptional RNAs protection.

Together these results show that the protective role of MTRES1 is not inhibitor specific but contributes to a general response to diminished mtDNA transcription. Moreover, they indicate that the MTRES1 protein acts at the transcriptional level and not through changes in mtDNA levels.

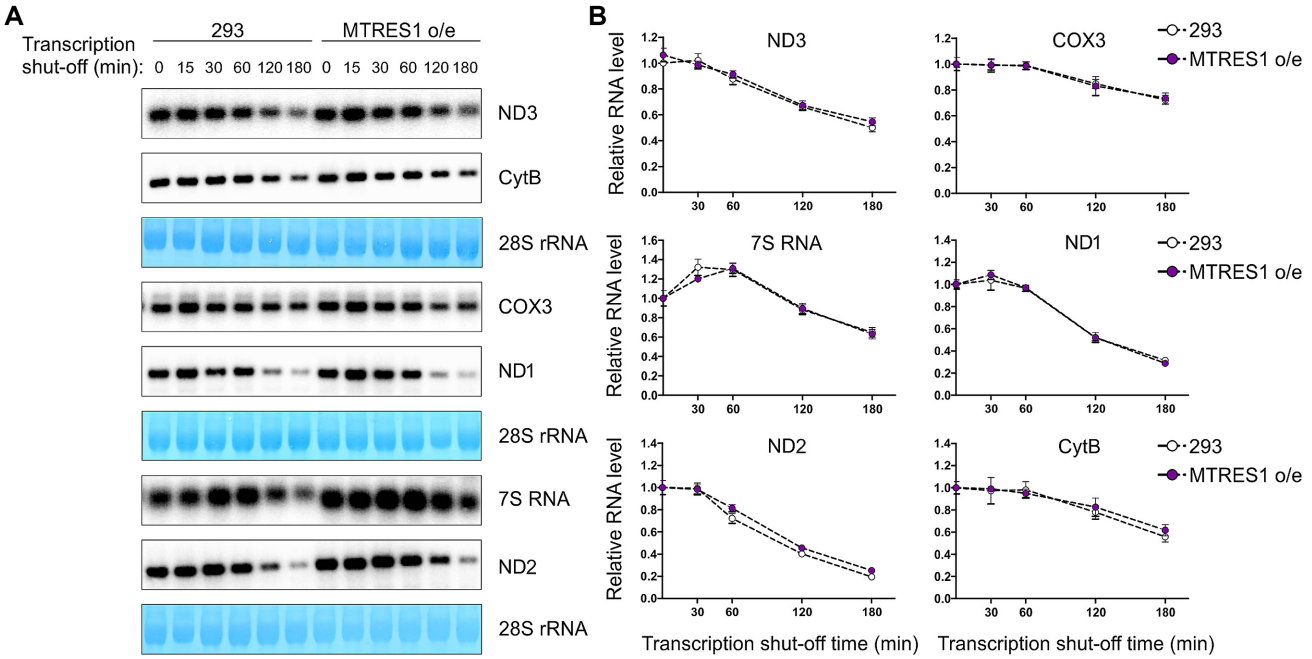

Figure 5. MTRES1 upregulation does not influence decay of mtRNAs. (**A** and **B**) Analysis of mtRNA stability. Parental 293 cells (293) or cells with upregulated level of MTRES1 (MTRES1 o/e) were treated with ActD (5 μg/μl) and collected after indicated time. Levels of mitochondrial transcripts were analyzed using northern blot (A). Four independent experiments were performed. Graphs show quantification of autoradiographs (mean ± SEM) (B).

The molecular function of MTRES1 strictly depends on its RNA-binding propensities

The observed transcription rescue along with the RNA-binding ability of MTRES1 prompted us to investigate whether the protective function of MTRES1 stems from its RNA binding activity. To this end, we first sought to design a mutated version of the protein with diminished RNA-binding activity, without compromising its overall structure. Structural studies of bacterial S4 proteins show an extensive RNA-binding surface, without pinpointing any single mutation that would disrupt the interaction (53,54), implying that disruption of RNA-binding ability of MTRES1 could require introduction of several mutations. We aligned the MTRES1 sequence to S4 proteins, which revealed a few highly conserved residues (Figure 6A). Next, we extracted the *Escherichia coli* S4 protein structure from the ribosome assembly structure (PDB ID: 4YBB) and searched for amino acids in proximity to RNA (Figure 6B). Based on that, we selected five residues in the MTRES1 sequence for alanine substitution (Figure 6A). The mutated protein was purified to high homogeneity (Supplementary Figure S10A) and subjected to electrophoretic mobility shift assay, which revealed significantly decreased affinity of the mutated protein toward 7S RNA substrate when compared with wild type (Figure 6C and D). Importantly, this decrease in affinity was not accompanied by overall misfolding of the mutated protein as multiangle light scattering and thermal shift assays showed that the mutant had the same biophysical properties as its wild-type counterpart (Supplementary Figure S10B and C). Thus, we concluded that the designed mutant indeed mimics the loss of RNA-binding ability of MTRES1.

We then obtained a stable 293 cell line in which endogenous MTRES1 was replaced by the FLAG-tagged RNA binding mutant protein. We confirmed the mitochondrial localization of the mutant protein and showed that its expression level was similar to the wild-type protein (Supplementary Figure S11A and B). We then checked whether the mutant can prevent loss of mtRNAs upon inhibition of mitochondrial transcription. We found that the mutated protein did not have the ability to prevent the decrease of 7S RNA level upon EtBr treatment (Figure 6E and F). Similarly, application of BrU labeling approach showed that the mutant was incapable of rescuing mitochondrial transcription that was challenged with EtBr treatment. Indeed, we observed a stronger loss of BrU signal upon EtBr treatment in parental or mutant upregulating cells in comparison to wild-type MTRES1-upregulating counterparts (Figure 6G).

These results show that elevated levels of wild-type MTRES1 but not of the RNA-binding mutant prevent mitochondrial transcription deficiency; therefore the protective role of MTRES1 involves its RNA-binding ability.

MTRES1 interacts with mitochondrial RNA polymerase and mitochondrial transcription initiation factor TFAM

To get an insight into the mechanism of the protective function of MTRES1 we used IP of MTRES1-EGFP to analyze its interaction with the mitochondrial transcription machinery constituents: mitochondrial RNA polymerase POLRMT and mitochondrial transcription initiation factor TFAM. We found enrichment of mitochondrial RNA polymerase in the MTRES1 IP fraction, while TFAM was present in the IP fractions but was not enriched in the

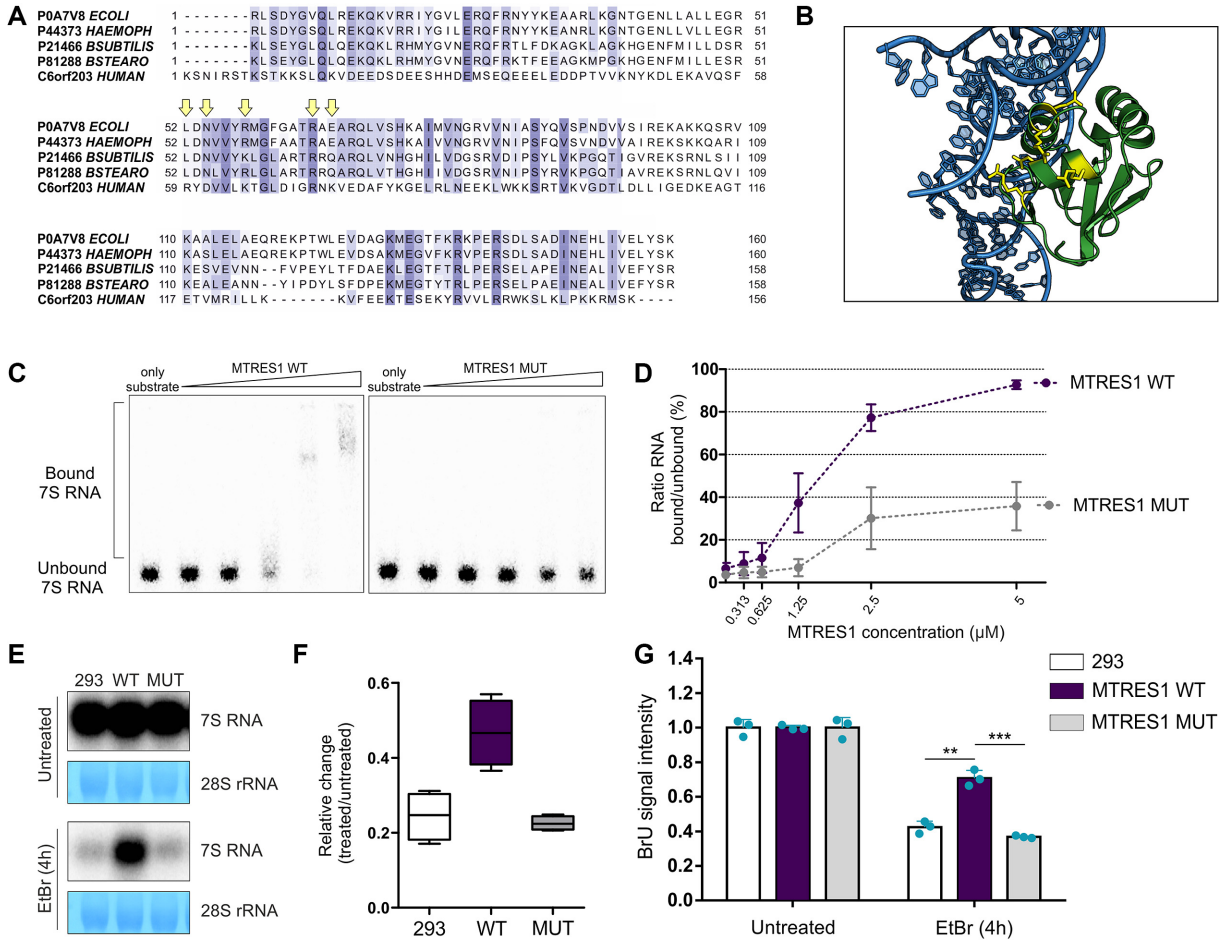

Figure 6. RNA-binding propensity is required for MTRES1 molecular function. (**A**) Sequence comparison of human MTRES1 and representative S4 proteins. Human- *Homo sapiens*, *E coli*- *Escherichia coli*, Haemoph- *Haemophilus influenzae*, Bsubtilis- *Bacillus subtilis*, Bstearo- *Geobacillus stearothermophilus*. Protein's Uniprot IDs are indicated. Conserved amino acids are highlighted in violet. Amino acids indicated with the arrows were selected for introduction of point mutations to obtain RNA-binding deficient mutant. For clarity only the region corresponding to mature MTRES1 is presented. (**B**) Structural representation of *E. coli* S4-protein (green). Amino acids indicated with arrows in panel A are marked in yellow while the RNA molecule is colored blue. The rendered structures originate from structure of the *E. coli* ribosome (PDB ID: 4YBB). (**C**) EMSA assay using *in vitro* transcribed 7S RNA substrate. The assay was performed using increasing concentrations of purified wild-type (MTRES1 WT) or RNA-binding deficient mutant (MTRES1 MUT) protein. (**D**) Quantification of EMSA results. Graph shows mean from three independent experiments ± SEM. (**E**) Northern blot analysis of 7S RNA levels of untreated and treated with EtBr parental 293 cells (293), cells overexpressing wild-type MTRES1 (WT) and cells overexpressing mutant MTRES1 (MUT). Methylene blue staining of nuclear-encoded rRNA serves as a loading control. (**F**) Quantification of northern blot results from four independent replicates. Relative change corresponding to 7S RNA level in untreated cells is shown. Boxes cover 25–75th percentiles. Whiskers go from smallest to largest values. Horizontal lines represent mean values. (**G**) Quantification of single-cell resolution fluorescence microscopy data. Mean intensity of mitochondrial BrU signal corresponding to nascent transcription events was calculated. Cells were treated for 4 h with EtBr. Individual values from the replicates are shown where in each replicate $n > 140$ cells were analyzed. Graphs show mean from the replicates ± SD. A two-tailed unpaired *t*-test was applied (**$P < 0.001$, ***$P < 0.0001$).

elution fraction as POLRMT was (Figure 7A). We observed MTRES1-POLRMT and MTRES1-TFAM interactions under normal as well as stress conditions (EtBr treatment). Importantly, we did not observe co-IP of POLRMT and TFAM in parental 293 cells or in the control cell line expressing mitochondrially targeted EGFP (mitoEGFP), showing specificity of the identified associations. Moreover, we did not detect highly abundant mitochondrial ribosomal proteins to co-purify with MTRES1 in the same IP samples (Supplementary Figure S2).

Next, we examined whether the observed interactions are direct or are mediated by RNA. To do so, we divided protein extracts into two equal fractions and treated one of them with RNase A prior to IP. Co-IP of POLRMT with MTRES1 turned out to be essentially insensitive to RNase treatment, indicating that interactions of MTRES1 with POLRMT are not mediated by RNA (Figure 7B). In contrast, the amount of TFAM in the elution fraction was strongly decreased when the protein lysate was treated with RNase before IP (Figure 7B), indicating that MTRES1 associates with TFAM in an RNA-dependent manner. In agreement with that MTRES1-TFAM interactions can be stabilized and become RNase A-insensitive if cells are subjected to chemical crosslinking with DSP (55) prior to cell lysis and IP (Figure 7C) since DSP introduces covalent bonds between proteins being in proximity.

In conclusion, MTRES1 physically interacts with POLRMT and TFAM *in vivo*, and the latter interaction is mostly

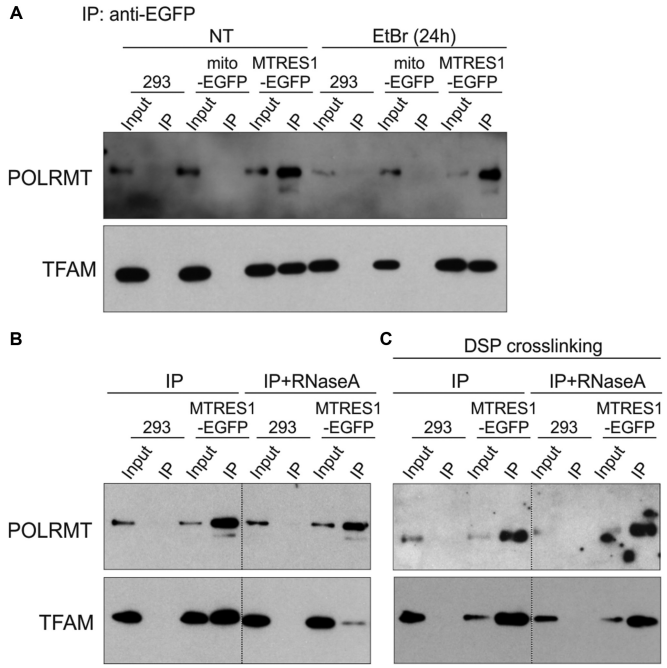

Figure 7. MTRES1 associates with mitochondrial transcription machinery. Western blot analysis of proteins co-immunoprecipitating with MTRES1. A cell line stably expressing MTRES1-EGFP was used. As a control parental 293 cells and/or the control cell line expressing mitochondrially targeted EGFP (mitoEGFP) were used. IP was performed with GFP-Trap nanobodies (Chromotek). Anti-POLRMT and anti-TFAM antibodies were used in western blot analysis. (**A**) Cells were treated (EtBr) or not (NT) with 100 ng/ml EtBr for 24 h followed by preparation of protein extracts and IP (**B**) Protein extracts were divided into two equal fractions and one of them was treated with RNase A prior to IP. (**C**) Cells were crosslinked with DSP prior to preparation of protein extracts. Protein extracts were divided into two equal fractions and one of them was treated with RNase A following IP.

RNA-mediated. These results further support the conclusion that MTRES1 plays its protective role at the transcriptional level, classifying it as mitochondrial transcription rescue factor (MTRES1).

DISCUSSION

Maintenance of mitochondrial gene expression is crucial for cellular homeostasis. In contrast to nuclear DNA, the mitochondrial genome exists in multiple copies. Expression of mitochondrially encoded genes seems to be correlated with mtDNA abundance (56); nevertheless, in some conditions a decrease in mtDNA levels can be compensated for at the transcriptional and/or post-transcriptional level. This compensation allows for maintenance of mitochondrial function despite severe depletion of mtDNA, as in the case of patients in whom mitochondrial disease develops late (57). Similarly, compensatory mechanism(s) acting at the RNA level operate during mammalian embryogenesis when transcription of mtDNA precedes its replication and is concomitant with a progressive reduction in mtDNA copies per cell (58–60). Compensation at the level of mtRNA metabolism has also been observed in *in vitro* cultured cells treated with mtDNA replication inhibitor (16). Molecular mechanisms and proteins involved in these compensatory pathways are largely unknown.

Here we present the results of a quantitative proteomic screen that revealed a new RNA binding protein C6orf203 as a factor engaged in mitochondrial transcription regulation upon perturbed mitochondrial gene expression. We show that C6orf203 is able to restore diminished transcription and that its level is upregulated upon depletion of mitochondrial nucleic acids, suggesting that it acts as a component of a compensatory mechanism that maintains proper function of mitochondria during stress. Our data suggest that the function of C6orf203 might be redundant during steady-state conditions. On the contrary during transcription arrest, C6orf203 functions as a protective factor to maintain proper mtRNAs level, thus we renamed the protein mitochondrial transcription rescue factor (MTRES1). MTRES1 acts at the transcription level and its protective function depends on its RNA binding ability. We found that MTRES1 restores mtRNAs levels in stress conditions without influencing their stability. According to our results, MTRES1 seems not to be a stable component of the mitochondrial ribosome, in agreement with previous reports suggesting that S4 protein is absent from the human mitochondrial ribosome (42–44). Nevertheless, we cannot exclude the possibility that MTRES1 may transiently or weakly associate with the mitochondrial ribosome.

MTRES1 clearly has a different impact on the mitochondrial transcriptome depending on the state and efficiency of mitochondrial transcription. We found that under steady-state conditions MTRES1 is required only for maintaining a proper level of 7S RNA, while the levels of other examined mtRNAs do not depend on MTRES1. Similarly, a screen for mtRNA processing factors performed by others did not reveal any significant changes in the processing or steady-state levels of coding and antisense mtRNAs (19) upon MTRES1 silencing; 7S RNA was not examined in the screen, precluding full comparison with our results (19). Our data support a view that 7S RNA is a separate transcriptional unit. Why its activity is affected by the knockdown of MTRES1 under normal conditions requires further studies. We observed that stability of 7S RNA does not depend on MTRES1, indicating that the protein is required for production of this transcript. In reference to our data, it seems that the impact of MTRES1 on the mitochondrial transcriptome is shifted to general response when mitochondrial transcription is affected. Under these conditions all examined mtRNAs benefit from the upregulation of MTRES1 as it prevents the decrease of mtRNAs levels by increasing mtDNA transcription.

In recent years biochemical and structural studies have provided substantial insight into the molecular mechanism of mtDNA transcription. These elegant studies showed that TFAM and TFB2M are required for the initiation of RNA synthesis, while the elongation factor TEFM supports polymerase processivity (15). Nevertheless, there are still open questions. For example, studies conducted so far did not consider stress conditions, which we addressed in our studies. We found that the support of mitochondrial transcription by MTRES1 requires its RNA binding properties.

Thus, it is possible that MTRES1 improves transcription by binding to nascent RNA when RNA polymerase is stalled. Bacterial S4 protein was shown to increase transcription by acting as an antitermination factor (61). The molecular details of this mechanism are unknown but it seems likely that it involves direct interaction of S4 protein with RNA polymerase (61). Murine C6orf203 was shown to be up-regulated *in vivo* in TFAM knockout mice (62), suggesting functional interplay between these proteins. Indeed, we observed that MTRES1 associates with TFAM in an RNA-dependent manner, which suggests weak/transient or indirect interactions. Moreover, we found that MTRES1 co-purifies with POLRMT. Interestingly, this interaction seems to be direct, as it is largely insensitive to RNase treatment. Association of MTRES1 with TFAM and POLRMT may indicate that it acts at the transcription initiation step as TFAM and POLRMT form the pre-initiation complex (15). Further biochemical and structural studies could test this hypothesis.

Recently, a study combining proteomic and transcriptomic approaches revealed activating transcription factor 4 (ATF4) to be a regulator of mitochondrial stress response (63). Since the MTRES1 protein is not present in this proteomic dataset it is not possible to assess to what extent MTRES1 contributes to the ATF4-regulated mechanism. The lack of MTRES1 in the abovementioned proteomic data suggests that this protein can be difficult to identify by a mass spectrometry approach. Accordingly in HeLa proteome MS-based studies MTRES1 sequence coverage was at 8% which put MTRES1 in the 12 percentile among ∼9000 quantified proteins (64). Such bias may explain why MTRES1 was not previously reported as an RNA-binding protein in various MS-based approaches (65–67). Our cross-linking and IP experiment as well as *in vitro* binding assays showed the RNA binding ability of MTRES1, as predicted based on the similarity to S4 proteins. Similarly to the work of others on S4 proteins (53–54), we were unable to pinpoint a single residue in MTRES1 that would be essential for interaction with RNA. Instead, we identified a few residues whose substitutions resulted in disruption of MTRES1-RNA interactions. Importantly, the structure of the protein was not disturbed by these substitutions, confirming that the mutated residues play a role in RNA binding. Our mutagenesis-based data pave the way for a detailed exploration of MTRES1 molecular function.

Since all proteins required for mtDNA maintenance and expression, including MTRES1, are encoded in the nucleus (3), cross-talk between mitochondria and the nucleus is necessary to coordinate nucleo-mitochondrial gene expression to maintain appropriate mitochondrial function (68). The murine C6orf203 gene was reported as potentially co-regulated in skeletal muscle (69) by PGC-1α, which is a key regulator of mitochondrial biogenesis in response to extracellular signals, cell energy demand, or mitochondrial dysfunction (70). It was shown that the expression of mitochondrial transcription machinery components including TFB2M and TFAM are regulated by the members of PGC-1 family (71,72). These observations, together with our data, suggest that MTRES1 may belong to a group of factors that adjust mtDNA expression to the cellular milieu.

DATA AVAILABILITY

PointBar is a software used to prepare bar charts with indicated individual values. PointBar tool is available at: http://adz.ibb.waw.pl/pointbar/. All scripts used in bioinformatics analyses are available for researchers upon request.

RNA-seq data obtained in this study is available in the GEO repository: GSE123683, [https://www.ncbi.nlm.nih.gov/geo/query/acc.cgi?&acc=GSE123683]. The mass spectrometry proteomics data have been deposited to the ProteomeXchange Consortium via the PRIDE (73) partner repository with the dataset identifier PXD012055, [https://www.ebi.ac.uk/pride/archive/projects/PXD012055]. Other relevant data are included in the paper and accompanying Supplementary Data or are available from the corresponding author upon reasonable request.

SUPPLEMENTARY DATA

Supplementary Data are available at NAR Online.

ACKNOWLEDGEMENTS

We thank Marcin Nowotny for help in structural analysis and Michal Malecki for critical reading. We thank Janina Durys and Gretchen Edwalds-Gilbert for proofreading the manuscript. We thank Dorota Adamska and Aleksander Chlebowski for technical support. Sequencing of N-terminus of polypeptide chains was performed by Biocentrum Sp. z o.o., Cracow.

Authors' contributions: AVK performed all experiments, performed DNA cloning, established stable cell lines, drafted the manuscript and prepared all figures under supervision of R.J.S. A.V.K. and R.J.S. designed experiments, had major contribution to data interpretation and preparation of the manuscript. D.C. performed mass spectrometry and proteins quantification. S.D.C. performed bioinformatic analysis of NGS data. Z.P. and A.V.K. purified recombinant proteins, designed mutant and conducted biophysical tests. L.S.B. contributed to high-throughput microscopy. A.D. contributed to manuscript preparation, provided laboratory infrastructure. R.J.S. conceived, designed and supervised the studies as well as contributed to organelles isolation. R.J.S. and A.V.K. analyzed data with contribution from all other authors.

FUNDING

National Science Centre, Poland [UMO-2014/12/W/NZ1/00463 to R.J.S.]; Foundation of Polish Science [TEAM TECH CORE FACILITY/2016-2/2]; European Union: the European Regional Development Fund [Innovative economy 2007–13, Agreement POIG.02.02.00-14-024/08-00]; Next Generation Sequencing Platform at the International Institute of Molecular and Cell Biology in Warsaw [6405/IA/1789/2014]. Funding for open access charge: National Science Centre, Poland [UMO-2014/12/W/NZ1/00463 to R.J.S.]; Foundation of Polish Science [TEAM TECH CORE FACILITY/2016-2/2].

Conflict of interest statement. None declared.

REFERENCES

1. Nicholls,T.J., Rorbach,J. and Minczuk,M. (2013) Mitochondria: mitochondrial RNA metabolism and human disease. *Int. J. Biochem. Cell Biol.*, **45**, 845–849.
2. Fernández-Silva,P., Enriquez,J.A. and Montoya,J. (2003) Replication and transcription of mammalian mitochondrial DNA. *Exp. Physiol.*, **88**, 41–56.
3. Schmidt,O., Pfanner,N. and Meisinger,C. (2010) Mitochondrial protein import: from proteomics to functional mechanisms. *Nat. Rev. Mol. Cell Biol.*, **11**, 655–667.
4. Calvo,S.E., Clauser,K.R. and Mootha,V.K. (2016) MitoCarta2.0: an updated inventory of mammalian mitochondrial proteins. *Nucleic Acids Res.*, **44**, D1251–D1257.
5. Van Haute,L., Pearce,S.F., Powell,C.A., D'Souza,A.R., Nicholls,T.J. and Minczuk,M. (2015) Mitochondrial transcript maturation and its disorders. *J. Inherit. Metab. Dis.*, **38**, 655–680.
6. Taylor,S.W., Fahy,E. and Ghosh,S.S. (2003) Global organellar proteomics. *Trends Biotechnol.*, **21**, 82–88.
7. Taylor,S.W., Fahy,E., Zhang,B., Glenn,G.M., Warnock,D.E., Wiley,S., Murphy,A.N., Gaucher,S.P., Capaldi,R.A., Gibson,B.W. *et al.* (2003) Characterization of the human heart mitochondrial proteome. *Nat. Biotechnol.*, **21**, 281–286.
8. Lotz,C., Lin,A.J., Black,C.M., Zhang,J., Lau,E., Deng,N., Wang,Y., Zong,N.C., Choi,J.H., Xu,T. *et al.* (2014) Characterization, design, and function of the mitochondrial proteome: from organs to organisms. *J. Proteome Res.*, **13**, 433–446.
9. Schweppe,D.K., Chavez,J.D., Lee,C.F., Caudal,A., Kruse,S.E., Stuppard,R., Marcinek,D.J., Shadel,G.S., Tian,R. and Bruce,J.E. (2017) Mitochondrial protein interactome elucidated by chemical cross-linking mass spectrometry. *Proc. Natl. Acad. Sci. U.S.A.*, **114**, 1732–1737.
10. Topf,U., Suppanz,I., Samluk,L., Wrobel,L., Böser,A., Sakowska,P., Knapp,B., Pietrzyk,M.K., Chacinska,A. and Warscheid,B. (2018) Quantitative proteomics identifies redox switches for global translation modulation by mitochondrially produced reactive oxygen species. *Nat. Commun.*, **9**, 324.
11. Floyd,B.J., Wilkerson,E.M., Veling,M.T., Minogue,C.E., Xia,C., Beebe,E.T., Wrobel,R.L., Cho,H., Kremer,L.S., Alston,C.L. *et al.* (2016) Mitochondrial protein interaction mapping identifies regulators of respiratory chain function. *Mol. Cell*, **63**, 621–632.
12. Anderson,S., Bankier,A.T., Barrell,B.G., de Bruijn,M.H., Coulson,A.R., Drouin,J., Eperon,I.C., Nierlich,D.P., Roe,B.A., Sanger,F. *et al.* (1981) Sequence and organization of the human mitochondrial genome. *Nature*, **290**, 457–465.
13. Ojala,D., Montoya,J. and Attardi,G. (1981) tRNA punctuation model of RNA processing in human mitochondria. *Nature*, **290**, 470–474.
14. Brzezniak,L.K., Bijata,M., Szczesny,R.J. and Stepien,P.P. (2011) Involvement of human ELAC2 gene product in 3′ end processing of mitochondrial tRNAs. *RNA Biol.*, **8**, 616–626.
15. Hillen,H.S., Temiakov,D. and Cramer,P. (2018) Structural basis of mitochondrial transcription. *Nat. Struct. Mol. Biol.*, **25**, 754–765.
16. Piechota,J., Szczesny,R., Wolanin,K., Chlebowski,A. and Bartnik,E. (2006) Nuclear and mitochondrial genome responses in HeLa cells treated with inhibitors of mitochondrial DNA expression. *Acta Biochim. Pol.*, **53**, 485–495.
17. Seidel-Rogol,B.L. and Shadel,G.S. (2002) Modulation of mitochondrial transcription in response to mtDNA depletion and repletion in HeLa cells. *Nucleic Acids Res.*, **30**, 1929–1934.
18. Liu,G., Mercer,T.R., Shearwood,A.-M.J., Siira,S.J., Hibbs,M.E., Mattick,J.S., Rackham,O. and Filipovska,A. (2013) Mapping of mitochondrial RNA-protein interactions by digital RNase footprinting. *Cell Rep.*, **5**, 839–848.
19. Wolf,A.R. and Mootha,V.K. (2014) Functional genomic analysis of human mitochondrial RNA processing. *Cell Rep.*, **7**, 918–931.
20. Arroyo,J.D., Jourdain,A.A., Calvo,S.E., Ballarano,C.A., Doench,J.G., Root,D.E. and Mootha,V.K. (2016) A genome-wide CRISPR death screen identifies genes essential for oxidative phosphorylation. *Cell Metab.*, **24**, 875–885.
21. Kuznetsova,I., Siira,S.J., Shearwood,A.-M.J., Ermer,J.A., Filipovska,A. and Rackham,O. (2017) Simultaneous processing and degradation of mitochondrial RNAs revealed by circularized RNA sequencing. *Nucleic Acids Res.*, **45**, 5487–5500.
22. Pearce,S.F., Rebelo-Guiomar,P., D'Souza,A.R., Powell,C.A., Van Haute,L. and Minczuk,M. (2017) Regulation of mammalian mitochondrial gene expression: recent advances. *Trends Biochem. Sci.*, **42**, 625–639.
23. Chevallet,M., Lescuyer,P., Diemer,H., van Dorsselaer,A., Leize-Wagner,E. and Rabilloud,T. (2006) Alterations of the mitochondrial proteome caused by the absence of mitochondrial DNA: a proteomic view. *Electrophoresis*, **27**, 1574–1583.
24. Szczesny,R.J., Kowalska,K., Klosowska-Kosicka,K., Chlebowski,A., Owczarek,E.P., Warkocki,Z., Kulinski,T.M., Adamska,D., Affek,K., Jedroszkowiak,A. *et al.* (2018) Versatile approach for functional analysis of human proteins and efficient stable cell line generation using FLP-mediated recombination system. *PLoS One*, **13**, e0194887.
25. Szczesny,R.J., Borowski,L.S., Brzezniak,L.K., Dmochowska,A., Gewartowski,K., Bartnik,E. and Stepien,P.P. (2010) Human mitochondrial RNA turnover caught in flagranti: involvement of hSuv3p helicase in RNA surveillance. *Nucleic Acids Res.*, **38**, 279–298.
26. Wessel,D. and Flügge,U.I. (1984) A method for the quantitative recovery of protein in dilute solution in the presence of detergents and lipids. *Anal. Biochem.*, **138**, 141–143.
27. Marchler-Bauer,A. and Bryant,S.H. (2004) CD-Search: protein domain annotations on the fly. *Nucleic Acids Res.*, **32**, W327–W331.
28. Chenna,R., Sugawara,H., Koike,T., Lopez,R., Gibson,T.J., Higgins,D.G. and Thompson,J.D. (2003) Multiple sequence alignment with the Clustal series of programs. *Nucleic Acids Res.*, **31**, 3497–3500.
29. Szczesny,R.J., Hejnowicz,M.S., Steczkiewicz,K., Muszewska,A., Borowski,L.S., Ginalski,K. and Dziembowski,A. (2013) Identification of a novel human mitochondrial endo-/exonuclease Ddk1/c20orf72 necessary for maintenance of proper 7S DNA levels. *Nucleic Acids Res.*, **41**, 3144–3161.
30. Pietras,Z. and PointBar (2018) doi:10.5281/zenodo.2150199.
31. Baughman,J.M., Nilsson,R., Gohil,V.M., Arlow,D.H., Gauhar,Z. and Mootha,V.K. (2009) A computational screen for regulators of oxidative phosphorylation implicates SLIRP in mitochondrial RNA homeostasis. *PLoS Genet.*, **5**, e1000590.
32. Sasarman,F., Brunel-Guitton,C., Antonicka,H., Wai,T., Shoubridge,E.A. and LSFC Consortium (2010) LRPPRC and SLIRP interact in a ribonucleoprotein complex that regulates posttranscriptional gene expression in mitochondria. *Mol. Biol. Cell*, **21**, 1315–1323.
33. Antonicka,H., Sasarman,F., Nishimura,T., Paupe,V. and Shoubridge,E.A. (2013) The mitochondrial RNA-binding protein GRSF1 localizes to RNA granules and is required for posttranscriptional mitochondrial gene expression. *Cell Metab.*, **17**, 386–398.
34. Wiese,S., Reidegeld,K.A., Meyer,H.E. and Warscheid,B. (2007) Protein labeling by iTRAQ: a new tool for quantitative mass spectrometry in proteome research. *Proteomics*, **7**, 340–350.
35. Gaucher,S.P., Taylor,S.W., Fahy,E., Zhang,B., Warnock,D.E., Ghosh,S.S. and Gibson,B.W. (2004) Expanded coverage of the human heart mitochondrial proteome using multidimensional liquid chromatography coupled with tandem mass spectrometry. *J. Proteome Res.*, **3**, 495–505.
36. Mahoney,D.W., Therneau,T.M., Heppelmann,C.J., Higgins,L., Benson,L.M., Zenka,R.M., Jagtap,P., Nelsestuen,G.L., Bergen,H.R. and Oberg,A.L. (2011) Relative quantification: characterization of bias, variability and fold changes in mass spectrometry data from iTRAQ-labeled peptides. *J. Proteome Res.*, **10**, 4325–4333.
37. Szymanski,M.R., Yu,W., Gmyrek,A.M., White,M.A., Molineux,I.J., Lee,J.C. and Yin,Y.W. (2017) A domain in human EXOG converts apoptotic endonuclease to DNA-repair exonuclease. *Nat. Commun.*, **8**, 14959.
38. Humble,M.M., Young,M.J., Foley,J.F., Pandiri,A.R., Travlos,G.S. and Copeland,W.C. (2013) Polg2 is essential for mammalian embryogenesis and is required for mtDNA maintenance. *Hum. Mol. Genet.*, **22**, 1017–1025.
39. Sato,T. and Mihara,K. (2010) Mammalian Oxa1 protein is useful for assessment of submitochondrial protein localization and mitochondrial membrane integrity. *Anal. Biochem.*, **397**, 250–252.
40. Sterky,F.H., Ruzzenente,B., Gustafsson,C.M., Samuelsson,T. and Larsson,N.-G. (2010) LRPPRC is a mitochondrial matrix protein that is conserved in metazoans. *Biochem. Biophys. Res. Commun.*, **398**, 759–764.

41. Shajani,Z., Sykes,M.T. and Williamson,J.R. (2011) Assembly of bacterial ribosomes. *Annu. Rev. Biochem.*, **80**, 501–526.
42. Cavdar Koc,E., Burkhart,W., Blackburn,K., Moseley,A. and Spremulli,L.L. (2001) The small subunit of the mammalian mitochondrial ribosome. Identification of the full complement of ribosomal proteins present. *J. Biol. Chem.*, **276**, 19363–19374.
43. Kaushal,P.S., Sharma,M.R., Booth,T.M., Haque,E.M., Tung,C.-S., Sanbonmatsu,K.Y., Spremulli,L.L. and Agrawal,R.K. (2014) Cryo-EM structure of the small subunit of the mammalian mitochondrial ribosome. *Proc. Natl. Acad. Sci. U.S.A.*, **111**, 7284–7289.
44. Amunts,A., Brown,A., Toots,J., Scheres,S.H.W. and Ramakrishnan,V. (2015) Ribosome. The structure of the human mitochondrial ribosome. *Science*, **348**, 95–98.
45. Jensen,K.B. and Darnell,R.B. (2008) CLIP: crosslinking and immunoprecipitation of in vivo RNA targets of RNA-binding proteins. *Methods Mol. Biol.*, **488**, 85–98.
46. Chacinska,A., Koehler,C.M., Milenkovic,D., Lithgow,T. and Pfanner,N. (2009) Importing mitochondrial proteins: machineries and mechanisms. *Cell*, **138**, 628–644.
47. Tomecki,R., Drazkowska,K., Kucinski,I., Stodus,K., Szczesny,R.J., Gruchota,J., Owczarek,E.P., Kalisiak,K. and Dziembowski,A. (2014) Multiple myeloma-associated hDIS3 mutations cause perturbations in cellular RNA metabolism and suggest hDIS3 PIN domain as a potential drug target. *Nucleic Acids Res.*, **42**, 1270–1290.
48. Park,C.B., Asin-Cayuela,J., Cámara,Y., Shi,Y., Pellegrini,M., Gaspari,M., Wibom,R., Hultenby,K., Erdjument-Bromage,H., Tempst,P. *et al.* (2007) MTERF3 is a negative regulator of mammalian mtDNA transcription. *Cell*, **130**, 273–285.
49. Terzioglu,M., Ruzzenente,B., Harmel,J., Mourier,A., Jemt,E., López,M.D., Kukat,C., Stewart,J.B., Wibom,R., Meharg,C. *et al.* (2013) MTERF1 binds mtDNA to prevent transcriptional interference at the light-strand promoter but is dispensable for rRNA gene transcription regulation. *Cell Metab.*, **17**, 618–626.
50. Zylber,E.A., Perlman,S. and Penman,S. (1971) Mitochondrial RNA turnover in the presence of cordycepin. *Biochim. Biophys. Acta*, **240**, 588–593.
51. Chrzanowska-Lightowlers,Z.M., Preiss,T. and Lightowlers,R.N. (1994) Inhibition of mitochondrial protein synthesis promotes increased stability of nuclear-encoded respiratory gene transcripts. *J. Biol. Chem.*, **269**, 27322–27328.
52. Piechota,J., Tomecki,R., Gewartowski,K., Szczesny,R., Dmochowska,A., Kudła,M., Dybczyńska,L., Stepien,P.P. and Bartnik,E. (2006) Differential stability of mitochondrial mRNA in HeLa cells. *Acta Biochim. Pol.*, **53**, 157–168.
53. Davies,C., Gerstner,R.B., Draper,D.E., Ramakrishnan,V. and White,S.W. (1998) The crystal structure of ribosomal protein S4 reveals a two-domain molecule with an extensive RNA-binding surface: one domain shows structural homology to the ETS DNA-binding motif. *EMBO J.*, **17**, 4545–4558.
54. Markus,M.A., Gerstner,R.B., Draper,D.E. and Torchia,D.A. (1998) The solution structure of ribosomal protein S4 delta41 reveals two subdomains and a positively charged surface that may interact with RNA. *EMBO J.*, **17**, 4559–4571.
55. Smith,A.L., Friedman,D.B., Yu,H., Carnahan,R.H. and Reynolds,A.B. (2011) ReCLIP (reversible cross-link immuno-precipitation): an efficient method for interrogation of labile protein complexes. *PLoS One*, **6**, e16206.
56. D'Erchia,A.M., Atlante,A., Gadaleta,G., Pavesi,G., Chiara,M., De Virgilio,C., Manzari,C., Mastropasqua,F., Prazzoli,G.M., Picardi,E. *et al.* (2015) Tissue-specific mtDNA abundance from exome data and its correlation with mitochondrial transcription, mass and respiratory activity. *Mitochondrion*, **20**, 13–21.
57. Barthélémy,C., Ogier de Baulny,H., Diaz,J., Cheval,M.A., Frachon,P., Romero,N., Goutieres,F., Fardeau,M. and Lombès,A. (2001) Late-onset mitochondrial DNA depletion: DNA copy number, multiple deletions, and compensation. *Ann. Neurol.*, **49**, 607–617.
58. Pikó,L. and Taylor,K.D. (1987) Amounts of mitochondrial DNA and abundance of some mitochondrial gene transcripts in early mouse embryos. *Dev. Biol.*, **123**, 364–374.
59. Thundathil,J., Filion,F. and Smith,L.C. (2005) Molecular control of mitochondrial function in preimplantation mouse embryos. *Mol. Reprod. Dev.*, **71**, 405–413.
60. Kameyama,Y., Filion,F., Yoo,J.G. and Smith,L.C. (2007) Characterization of mitochondrial replication and transcription control during rat early development in vivo and in vitro. *Reprod. Camb. Engl.*, **133**, 423–432.
61. Torres,M., Condon,C., Balada,J.M., Squires,C. and Squires,C.L. (2001) Ribosomal protein S4 is a transcription factor with properties remarkably similar to NusA, a protein involved in both non-ribosomal and ribosomal RNA antitermination. *EMBO J.*, **20**, 3811–3820.
62. Kühl,I., Miranda,M., Atanassov,I., Kuznetsova,I., Hinze,Y., Mourier,A., Filipovska,A. and Larsson,N.-G. (2017) Transcriptomic and proteomic landscape of mitochondrial dysfunction reveals secondary coenzyme Q deficiency in mammals. *Elife*, **6**, e30952.
63. Quirós,P.M., Prado,M.A., Zamboni,N., D'Amico,D., Williams,R.W., Finley,D., Gygi,S.P. and Auwerx,J. (2017) Multi-omics analysis identifies ATF4 as a key regulator of the mitochondrial stress response in mammals. *J. Cell Biol.*, **216**, 2027–2045.
64. Hein,M.Y., Hubner,N.C., Poser,I., Cox,J., Nagaraj,N., Toyoda,Y., Gak,I.A., Weisswange,I., Mansfeld,J., Buchholz,F. *et al.* (2015) A human interactome in three quantitative dimensions organized by stoichiometries and abundances. *Cell*, **163**, 712–723.
65. Castello,A., Fischer,B., Eichelbaum,K., Horos,R., Beckmann,B.M., Strein,C., Davey,N.E., Humphreys,D.T., Preiss,T., Steinmetz,L.M. *et al.* (2012) Insights into RNA biology from an atlas of mammalian mRNA-binding proteins. *Cell*, **149**, 1393–1406.
66. Beckmann,B.M., Horos,R., Fischer,B., Castello,A., Eichelbaum,K., Alleaume,A.-M., Schwarzl,T., Curk,T., Foehr,S., Huber,W. *et al.* (2015) The RNA-binding proteomes from yeast to man harbour conserved enigmRBPs. *Nat. Commun.*, **6**, 10127.
67. Bao,X., Guo,X., Yin,M., Tariq,M., Lai,Y., Kanwal,S., Zhou,J., Li,N., Lv,Y., Pulido-Quetglas,C. *et al.* (2018) Capturing the interactome of newly transcribed RNA. *Nat. Methods*, **15**, 213–220.
68. Garesse,R. and Vallejo,C.G. (2001) Animal mitochondrial biogenesis and function: a regulatory cross-talk between two genomes. *Gene*, **263**, 1–16.
69. Nsiah-Sefaa,A., Brown,E.L., Russell,A.P. and Foletta,V.C. (2014) New gene targets of PGC-1α and ERRα co-regulation in C2C12 myotubes. *Mol. Biol. Rep.*, **41**, 8009–8017.
70. Jones,A.W.E., Yao,Z., Vicencio,J.M., Karkucinska-Wieckowska,A. and Szabadkai,G. (2012) PGC-1 family coactivators and cell fate: roles in cancer, neurodegeneration, cardiovascular disease and retrograde mitochondria-nucleus signalling. *Mitochondrion*, **12**, 86–99.
71. Wu,Z., Puigserver,P., Andersson,U., Zhang,C., Adelmant,G., Mootha,V., Troy,A., Cinti,S., Lowell,B., Scarpulla,R.C. *et al.* (1999) Mechanisms controlling mitochondrial biogenesis and respiration through the thermogenic coactivator PGC-1. *Cell*, **98**, 115–124.
72. Gleyzer,N., Vercauteren,K. and Scarpulla,R.C. (2005) Control of mitochondrial transcription specificity factors (TFB1M and TFB2M) by nuclear respiratory factors (NRF-1 and NRF-2) and PGC-1 family coactivators. *Mol. Cell Biol.*, **25**, 1354–1366.
73. Perez-Riverol,Y., Csordas,A., Bai,J., Bernal-Llinares,M., Hewapathirana,S., Kundu,D.J., Inuganti,A., Griss,J., Mayer,G., Eisenacher,M. *et al.* (2018) The PRIDE database and related tools and resources in 2019: improving support for quantification data. *Nucleic Acids Res.*, **47**, D442–D450.